Title

Synthesis, structural characterization, and luminescence properties of mono- and di-nuclear platinum(II) complexes containing 2-(2-pyridyl)-benzimidazole

Authors

Niknam, Fatemeh
Hamidizadeh, Peyman
Nabavizadeh, S Masoud
et al.

Publication Date

2019-12-01

DOI

10.1016/j.ica.2019.119133

Synthesis, Structural Characterization, and Luminescence Properties of Mono- and Di-Nuclear Platinum(II) Complexes Containing 2-(2-Pyridyl)-benzimidazole

Fatemeh Niknam,[a†] Peyman Hamidizadeh,[a†] S. Masoud Nabavizadeh,*[a,b] Fatemeh Niroomand Hosseini,[c] S. Jafar Hoseini,[a] Peter C. Ford[b] and Mahdi M. Abu-Omar*[b]

[a]*Professor Rashidi Laboratory of Organometallic Chemistry, Department of Chemistry, College of Sciences, Shiraz University, Shiraz, 71467-13565, Iran,* [b]*Department of Chemistry and Biochemistry, University of California, Santa Barbara, Santa Barbara, California 93106, United States.* [c]*Department of Chemistry, Shiraz Branch, Islamic Azad University, Shiraz 71993–37635, Iran*

[†] Both authors contributed equally to this work.

Corresponding Author: S. Masoud Nabavizadeh (nabavizadeh@shirazu.ac.ir), Mahdi Abu-Omar (abuomar@chem.ucsb.edu)

Abstract

The starting complex [Pt(Me)(DMSO)(pbz)], (**1**, pbz = 2-(2-pyridyl)benzimidazolate) was prepared by a known method using the

reaction of $[Pt(Me)_2(DMSO)_2]$, **A**, with Hpbz at room temperature. Reaction of **1** with an equivalent of a phosphine ligand gave the neutral mononuclear complexes [Pt(Me)(L)(pbz)], (**2**, (L = PPh_3) or and **3**, (L =PPh_2Me**)**. Reaction of **1** with 0.5 equivalent of the linear diphosphine 1,1'–bis(diphenylphosphino)acetylene (dppac) gave the binuclear complex $[Pt_2(Me)_2(\mu\text{-dppac})(pbz)_2]$, **4**. All Each the complexes were was fully characterized by NMR spectroscopy, X-ray crystallography and mass spectrometry. The photophysical properties of the complexes were investigated in under different conditions and interpretation was, supported by TD-DFT calculations. The low-lying transitions in the absorption and emission spectra were assigned as having LLCT/MLCT (ligand to ligand charge transfer/metal-to-ligand charge transfer) character. We also describe the luminescence properties of $[Pt(Me)(PPh_3)(ppy)]$, **7**, and $[Pt(Me)(PPh_2Me)(ppy)]$, **8**, (ppy is 2-phenylpyridinate), the (N^C^-) analogues of **2** and **3**.

Keywords: Platinum; Organometallic compounds; Crystal structure; Photophysics.

Introduction

POrganometallic latinum and other heavier metal complexes of polydentate aromatic nitrogen and orthometallated ligands have attracted considerable attention because of their severalowing to potential photooptical and therapeutic applications in chemistry and industry [1-5]. Among different classes of transition metal complexesThese include, phosphorescent organotransition metal compounds have been widely investigated asthat can serve as efficient emitters in optoelectronic devices [6, 7] and molecular sensors [8-10] owing to their high luminescence quantum yields [11-16]. Of particular interest are Pt(II) complexes of strong field ligands like benzo[h]quinolinate (bhq) and 2-phenylpyridinate (ppy-) [17-23]. Additionally, cycloplatinated(II) complexes bearing the rollover 2,2′-bipyridinate (bpy) ligand can also be emissive in solution or solid state [24-26]. Among the reported emissive Pt(II) compounds, those with the [Pt(C^N)R] moiety (C^N= cyclometalated ligand and R= alkyl, aryl or halide) are very attractive due to their ease of preparation [22, 25, 27, 28]. These cyclometalated Pt(II) complexes have been synthesized through a C-H activation of ligands C^N (such as ppy, bpy and bhq) with a suitable Pt(II) precursor complex [19, 29-31].

The 2-(2-pyridyl)benzimidazole ligand (Hpbz, see Chart 1) has been used as *N*,*N*′-diimine chelating ligand in coordination chemistry [32-36]. The ease of synthesis and the commercial availability of Hpbz are the factors that make this an attractive ligand for coordination to metals.

Complexes of Hpbz have been prepared through N-H bond activation of the imidazole unit (instead of C-H activation in Hppy and Hbhq ligands), converting the ligand from neutral to anionic forms.

Although there are many reports on photophysical properties of C^N ~~(= bpy, ppy or bhq)~~ transition metal complexes~~,[22, 26, 37-39]~~ [22, 26, 37-39], the photophysical properties of the platinum(II) complexes of pbz– have not been widely explored [40-44]. Haga demonstrated [45] that $[Ru(bpy)_2(pbz)]^{2+}$ shows ^{3}MLCT luminescence comparable to that of $[Ru(bpy)_3]^{2+}$, although slightly red-shifted and with a slightly reduced lifetime. Hpbz derivatives have been also used as 'bipyridine analogues' in a variety of complexes with metal ions such as Cu(I)~~,[46]~~ [46], Cu(II~~),[47]~~) [47], Zn(II) ~~,~~[47], Ru(II~~),[48]~~) [48], Os(II~~),[49]~~) [49] and Re(I) [50, 51]. Ward et. al. reported [52] a series of Pt(II) complexes of general formula $[Pt(R\text{-}pbz)(CCR)_2]$ (where R-pbz is alkylated 2-(2-pyridyl)benzimidazole and –CCR is an acetylide ligand). These complexes showed luminescence in the range 553–605 nm arising from the ^{3}MLCT (metal to ligand charge transfer) state, with lifetimes of up to 500 ns and quantum yields of up to 6% in air-saturated CH_2Cl_2 at room temperature. The syntheses of luminescent organic molecules based on the 2-(2-pyridyl)benzimidazolyl chromophore have been reported by Wang and coworkers [42]. These ligands coordinate to the Pt(II) center readily *via* N,N-chelation to form mononuclear, dinuclear, and trinuclear Pt(II) complexes that show orange/red emissions at 77 K in a frozen solution or in the solid state, attributed to ~~metal to ligand charge transfer (~~MLCT~~) ~~transitions.

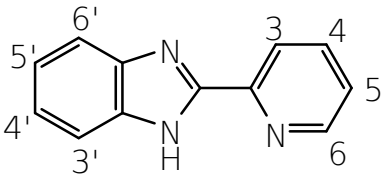

Chart1. Structure of Hpbz with NMR labeling

Herein, we report the synthesis, characterization and photophysical properties of a series of mono- and di-nuclear Pt(II) complexes of pbz^- and various mono- or bis-phosphine ligands. In addition, TD-DFT calculations were carried out in order to gain better insight into the nature of the photoluminescent excited states.

Experimental section

~~General remarks~~Instruments and techniques

The ^1H and ^{31}P NMR spectra were recorded in $CDCl_3$ solutions on a Bruker Avance DPX 400 MHz spectrometer using TMS (^1H) and H_3PO_4 (^{31}P) as references. All chemical shifts and coupling constants are in ppm and Hz, respectively. Microanalyses were performed using a Thermo Finnigan Flash EA-1112 CHNSO rapid elemental analyzer and melting points were recorded on a Buchi 530 apparatus. UV-vis absorption spectra were recorded on a PerkinElmer Lambda 25 spectrophotometer using a cuvette with a path length of 1 cm and/or 1 mm. Excitation and emission spectra were obtained on a PerkinElmer LS45 fluorescence spectrometer with the lifetimes measured in phosphorimeter mode. Absolute measurements of the photoluminescence quantum yield at ambient temperature were performed using a C9920-02 (Hamamatsu Photonics) system equipped with a Spectralon® integrating sphere.

~~The precursor complex, $[Pt(Me)_2(DMSO)_2]$, **A**, was prepared by the literature method.[53] Bis(diphenylphosphino)acetylene (dppac), 2-(2-pyridyl) benzimidazole (Hpbz), PPh_2Me and PPh_3 were purchased from commercial sources. The ^1H NMR labeling for the pbz ligand is shown in Chart 1 for clarifying the chemical shift assignments.~~

Synthesis of Pt complexes

The precursor complex, $[Pt(Me)_2(DMSO)_2]$, **A**, was prepared by the literature method.[53] Bis(diphenylphosphino)acetylene (dppac), 2-(2-pyridyl) benzimidazole (Hpbz), PPh_2Me and PPh_3 were purchased from commercial sources. The ^1H NMR labeling for the pbz ligand is shown in Chart 1 for clarifying the chemical shift assignments.

[Pt(Me)(DMSO)(pbz)], 1

A previously reported method [41] was used for preparation of this complex with different solvents such as acetone, chloroform and diethyl ether instead of CH_2Cl_2. Hpbz (51.2 mg, 0.26 mmol) was added to a solution of **A** (100 mg, 0.26 mmol) in 20 mL diethyl ether. The solution was stirred at room temperature for 2 h and then the solvent was removed by evaporation. The yellow residue was washed with ether to give the final product **1**. Yield: 75%. Anal. Calc. for $C_{15}H_{17}N_3SOPt$: C, 37.3; H, 3.5; N, 8.7%, Found: C, 37.4; H, 3.6; N, 8.5%. ^1H NMR in $CDCl_3$: δ 1.25 [s, $^2J_{PtH}$ = 79.6 Hz, 3H, Me]; 3.44 [s, $^3J_{PtH}$ = 31.5 Hz, 6H, DMSO]; 7.17 [m, 2H, $H^{5'}$and $H^{4'}$]; 7.35 [t, $^3J_{HH}$ = 12.8 Hz, 1H, H^5]; 7.80 [d, $^3J_{HH}$ = 7.7 Hz, 1H,

$H^{6'}$]; 7.86 [d, $^3J_{HH}$ = 8.2 Hz, 1H, $H^{3'}$]; 7.95 [t, $^3J_{HH}$ = 15.1 Hz, 1H, H^4]; 8.38 [d, $^3J_{HH}$ = 7.8 Hz, 1H, H^3]; 9.58 [d, $^3J_{PtH}$ = 15.0 Hz, $^2J_{HH}$ = 5.4 Hz, 1H, H^6].

[Pt(Me)(PPh_3)(pbz)], 2

PPh_3 (54.4 mg, 0.21 mmol) was added to a solution of **1** (100 mg, 0.21 mmol) in acetone (20 mL). This was stirred at room temperature for 4 h and then the solvent was removed by evaporation. The yellow residue was washed with cold diethyl ether to remove the impurities and to give **2** (72.2 mg). Yield: 46%; m.p. > 250 °C. Anal: Calc. for $C_{31}H_{26}N_3PPt$: C, 55.8; H, 3.9; N, 6.3%, Found: C, 56.1; H, 3.8; N, 6.1%. NMR in $CDCl_3$: δ(^{1}H) 1.22 [d, $^2J_{PtH}$ = 78.5 Hz, $^3J_{PH}$ = 4.7 Hz, 3H, Me ligand *trans* to N of 2-pyridyl ring]; 6.64 [t, $^3J_{HH}$ = 11.9 Hz, 1H, H^5]; 7.15, [m, 2H, $H^{5'}$and $H^{4'}$]; 7.44 and 7.83 [m, Ph of PPh_3]; 7.98 [d, $^3J_{HH}$ = 7.9 Hz, 1H, H^3]; 8.40 [d, $^3J_{HH}$ = 8.1 Hz, 1H, H^6]. δ(^{31}P) 21.5 [s, $^1J_{PtP}$ = 4178 Hz, 1P]. ESI-TOF-MS: m/z 667.15 [**2** + H]$^+$.

[Pt(Me)(PPh_2Me)(pbz)], 3

PPh_2Me (39 mL, 0.21 mmol) was added to a solution of **1** (100 mg, 0.21 mmol) in acetone (20 ml) and the solution was stirred at room temperature for 4 h. The solvent was evaporated and the yellow residue was washed with cold diethyl ether to give complex **3** (79.5 mg). Yield: 56%; m.p. = 240 °C (decomp.). Anal. Calc. for $C_{26}H_{24}N_3PPt$: C, 51.6; H, 4.0; N, 6.9%, Found: C, 51.3; H, 3.8; N, 6.6%. NMR in $CDCl_3$: δ(^{1}H) 1.38 [d, $^2J_{PtH}$ = 76.6 Hz, $^3J_{PH}$ = 5.3 Hz, 3H, Me ligand *trans* to N of 2-pyridyl ring]; 2.20 [d, $^3J_{PtH}$ = 42.4 Hz, $^3J_{PH}$ = 9.8 Hz, 3H, Me of PPh_2Me ligand]; 6.64 [td, $^3J_{HH}$ = 13.2 Hz, $^4J_{HH}$ = 1.5 Hz, 1H, H^5]; 7.15 [m, 2H, $H^{5'}$ and $H^{4'}$]; 7.47 and 7.78 [m, Ph of PPh_2Me]; 7.82 [d, $^3J_{HH}$ = 8.1 Hz, 1H, H^4]; 8.01 [d, $^3J_{HH}$ = 7.7 Hz, 1H, H^3];

8.35 [d, $^{3}J_{HH}$ = 8.6 Hz, 1H, H^{6}]. δ(^{31}P) 2.4 [s, $^{1}J_{PtP}$ = 4055 Hz, 1P]. ESI-TOF-MS: m/z 605.14 [**3** + H]$^{+}$.

[$Pt_2(Me)_2$(μ-dppac)$(pbz)_2$], 4

Bis(diphenylphosphino)acetylene (41 mg, 0.10 mmol) was added to a solution of **1**, (100 mg, 0.21 mmol) in acetone (20 ml). This was stirred at room temperature for 4 h and then the solvent was removed by evaporation. The yellow residue was washed with cold diethylether to remove the impurities and to give **4** (80 mg). Yield: 57%; m.p. > 250 °C. Anal. Calc. for $C_{52}H_{42}N_6P_2Pt_2$, C, 51.9; H, 3.5; N, 7.0%, Found, C, 51.5; H, 3.5; N, 6.7%. NMR in $CDCl_3$: δ(^{1}H) 1.26 [d, $^{2}J_{PtH}$ = 75.6 Hz, $^{3}J_{PH}$ = 6.0 Hz, 6H, Me ligands *trans* to N of 2-pyridyl ring]; 6.63 [t, $^{3}J_{HH}$ = 12.7 Hz, 1H, H^{5}]; 7.15 [t, $^{3}J_{HH}$ = 15.4 Hz, 1H, $H^{5'}$]; 7.22 and 7.44 [t, $^{3}J_{HH}$ = 14.5 Hz, 1H, $H^{4'}$]; 7.52-7.58 [m, $H^{6'}$and $H^{3'}$]; 7.77 [m, Ph of dppac]; 7.86 [$^{3}J_{HH}$ = 8.7 Hz, 1H, H^{4}]; 7.93 [$^{3}J_{HH}$ = 7.6 Hz, 1H, H^{3}]; 8.36 [$^{3}J_{PtH}$ = 34 Hz, $^{4}J_{PH}$ = 8.4 Hz, 1H, H^{6}]. δ(^{31}P) -0.03 [s, $^{1}J_{PtP}$ = 4207 Hz]. ESI-TOF-MS: m/z 1203.23 [**4** + H]$^{+}$.

Crystallographic data

Single crystal X-ray diffraction data for complexes **1-4** were collected on a Bruker KAPPA APEX II diffractometer equipped with an APEX II CCD detector using a TRIUMPH monochromator with a Mo Kα X-ray source (k = 0.71073 Å). The crystals were mounted on a cryoloop under Paratone-N oil and kept under nitrogen. Absorption correction of the data was carried out using the multiscan method SADABS.[54] Subsequent calculations were carried out using SHELXTL.[55] Structure determination was done using intrinsic methods. Structure solution, refinement, and creation of publication data was performed using SHELXTL.

Crystallographic information is presented in Table 1. Crystallographic data for the structural analysis has been deposited with the Cambridge Crystallographic Data Centre, No. CCDC 1571934 (**1**), 1571935 (**2**), 1874223 (**3**) and 1874224 (**4**). Copies of this information may be obtained free of charge from: The Director, CCDC, 12 Union Road, Cambridge, CB2 1EZ, UK. Fax: +44(1223)336-033, e-mail: deposit@ccdc.cam.ac.uk, or www.ccdc.cam.ac.uk.

Table 1. Crystal and structure refinement for complexes **1**-**4**.

	1.$CHCl_3$	**2**	**3**.CH_2Cl_2	**4**
Empirical formula	$C_{16}H_{18}Cl_3N_3OPtS$	$C_{31}H_{26}N_3PPt$	$C_{27}H_{26}Cl_2N_3PPt$	$C_{52}H_{42}N_6P_2Pt_2$
Formula weight	601.83	666.61	689.47	1203.03
Temperature (K)	100(2)	100(2)	125(2)	100(2)
Wavelength(Å)	0.71073	0.71073	0.71073	0.71073
Crystal system	Monoclinic	Monoclinic	Monoclinic	Monoclinic
Space group	C2/c	$P2_1$	$P2_{1/C}$	$P2_{1/n}$
Unit cell dimensions				
a/Å	28.732(12)	8.2967(11)	10.027(5)	8.275(5)
b/Å	9.095(3)	18.561(2)	16.815(10)	25.122(14)
c/Å	15.149(5)	9.1728(17)	15.551(9)	10.608(8)
ß/°	98.994(10)	116.883(3)	104.504(13)	97.94(3)
VolumeÅ^3	3911(2)	1259.9(3)	2538(2)	2184(2)
Z	8	2	4	2
Density (calculated)/ Mg/m^3	2.044	1.757	1.804	1.829
Absorption coefficient/m m^{-1}	7.702	5.658	5.823	6.516
F(000)	2304	652	1344	1164
Theta range	1.435 to	2.194 to	1.816 to	1.621 to

for data collection	27.251°	27.159°	26.674°	27.049°
Reflections collected	8746	12076	10796	9894
Independent reflections, [R(int)]	4282, [0.0604]	5501, [0.0233]	5277, [0.0634]	4680, [0.0490]
Max. and min. transmission	0.7455 and 0.5397	0.7455 and 0.6630	0.7454 and 0.6628	0.7455 and 0.5174
Data / restraints / parameters	4282 / 0 / 224	5501 / 1 / 326	5277 / 0 / 309	4680 / 0 / 281
Goodness-of-fit on F^2	0.845	1.026	0.972	1.019
R1/wR2 [I>2sigma(I)]	0.0458/0.1078	0.0208/0.0391	0.0435/0.0763	0.0418/0.0843

Computational details

Gaussian 09 was used [56] to fully optimize all the structures at the B3LYP level of density functional theory. The effective core potential of Hay and Wadt with a double-ξ valence basis set (LANL2DZ) was chosen to describe Pt [57]. The 6-31G(d) basis set was used for all other atoms. To evaluate and ensure the optimized structures of the molecules, frequency calculations were carried out using analytical second derivatives. In all cases only real frequencies were obtained for the optimized structures. The calculations for the electronic absorption spectra by time-dependent DFT (TD-DFT) were performed at the same level of theory. The compositions of molecular orbitals and theoretical absorption spectra were plotted using the “Chemissian” software [58].

Results and Discussion

Synthesis of the complexes

The synthetic routes for complexes **2-4** are shown in Scheme 1. The precursor complex [Pt(Me)(DMSO)(pbz)], **1**, was prepared through the reaction of [$Pt(Me)_2(DMSO)_2$], **A**, with Hpbz in 1:1 ratio. Complexes [Pt(Me)(PPh_3)(pbz)], **2**, and [Pt(Me)(PPh_2Me)(pbz)], **3**, were prepared via reaction of **1** with PPh_3 and PPh_2Me in 1:1 ratio, respectively. In this context, the reaction of **1** with 0.5 equivalent of dppac (bis(diphenylphosphino)acetylene) ligand resulted in the formation of the dinuclear complex [$Pt_2(Me)_2$(dppac)$(pbz)_2$], **4**.

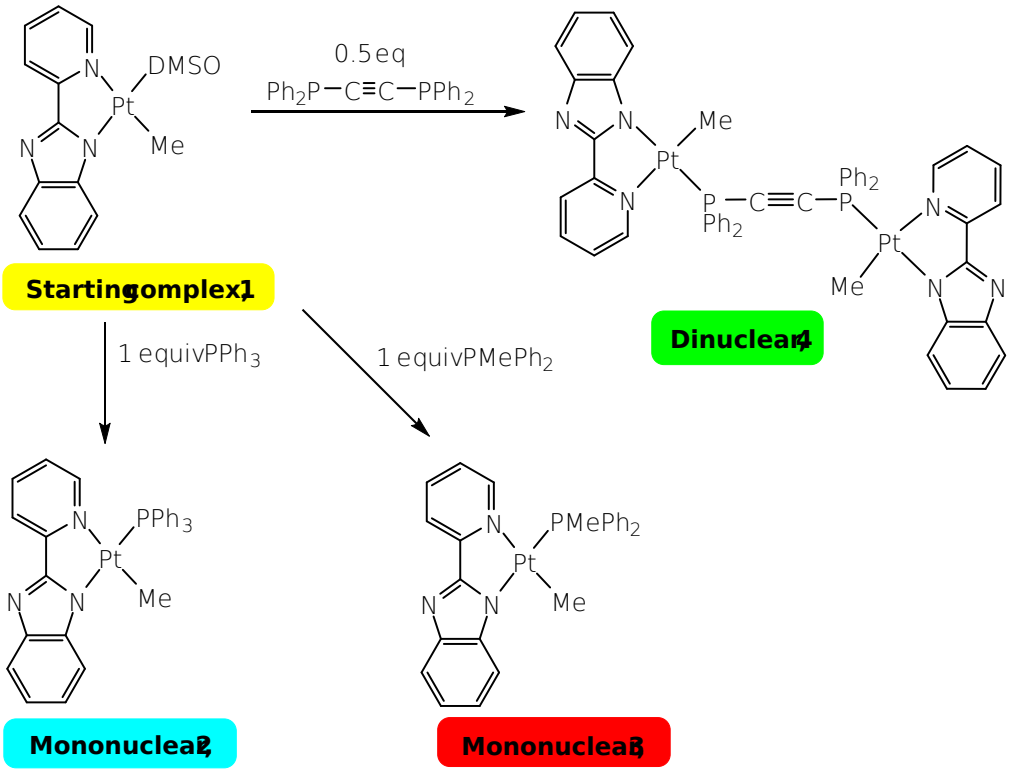

Scheme 1. Preparation of Pt complexes **2-4**

Characterization of the complexes

The structures of new complexes were fully characterized using multinuclear NMR spectroscopy (^1H and $^{31}P\{^1H\}$ NMR), UV-vis spectroscopy, electrospray ionization mass spectroscopy (ESI-MS),

fluorescence spectroscopy, X-ray crystallography and elemental analysis. The $^{31}P\{^{1}H\}$ NMR spectra are illustrated in Fig. 1 (details of the numerical NMR data are collected in the Experimental section). For **2** and **3**, singlet signals were observed at δ = 21.5 ($^{1}J_{PtP}$ = 4178 Hz) and 2.4 ($^{1}J_{PtP}$ = 4055 Hz), respectively, and assigned to the phosphorus atom *trans* to N of benzimidazole ring. For the dimeric complex **4**, the $^{31}P\{^{1}H\}$ NMR spectrum of the symmetrical dppac-bridged complex exhibits a singlet at δ = –0.03 flanked by ^{195}Pt satellites with $^{1}J_{PtP}$ = 4207 Hz. The presence of a single signal for dppac ligand is indicative of a symmetrical bridge between two PtMe(pbz) moieties. Each P atom is located *trans* to the ligating N atom of the benzimidazole ring of the pbz ligand. Correspondingly, each Me ligand is thus located *trans* to the ligating N atom of pyridyl ring. In the ^{1}H NMR spectrum of **2**, replacement of DMSO by PPh_3 results in significant upfield shifts were observed for H^6 (from 9.58 to 8.40 ppm) and H^3 (from 8.38 to 7.98 ppm) compared to **1**. A similar shift was also observed for the pyridyl proton of H^5 (from 7.35 to 6.64 ppm) as well as other aromatic protons in benzimidazole moiety. A similar behavior was observed in the ^{1}H NMR spectra for complex **3** when compared to complex **1**. The ^{1}H NMR spectrum of **3**, also contains two important signals at δ = 1.38 (with $^{2}J_{PtH}$ = 76.6 Hz and $^{3}J_{PH}$ = 5.3 Hz) and δ =2.20 (with $^{3}J_{PtH}$ = 42.4 Hz and $^{3}J_{PH}$ = 9.8 Hz), related to Me ligand *trans* to ligating N atom of pyridyl ring and Me group in PPh_2Me ligand, respectively. In the ^{1}H NMR spectrum of **4**, in $CDCl_3$ at room temperature, the signal for Pt-Me group appeared at δ = 1.26 ppm as a doublet due to the coupling to phosphorus (with $^{3}J_{PH}$ = 6.0 Hz). This signal is further coupled to ^{195}Pt (with $^{2}J_{PtH}$ = 75.6 Hz) confirming

that the methyl ligands are located *trans* to aromatic N atoms, which is a characteristic value for Me ligand *trans* to N [59].

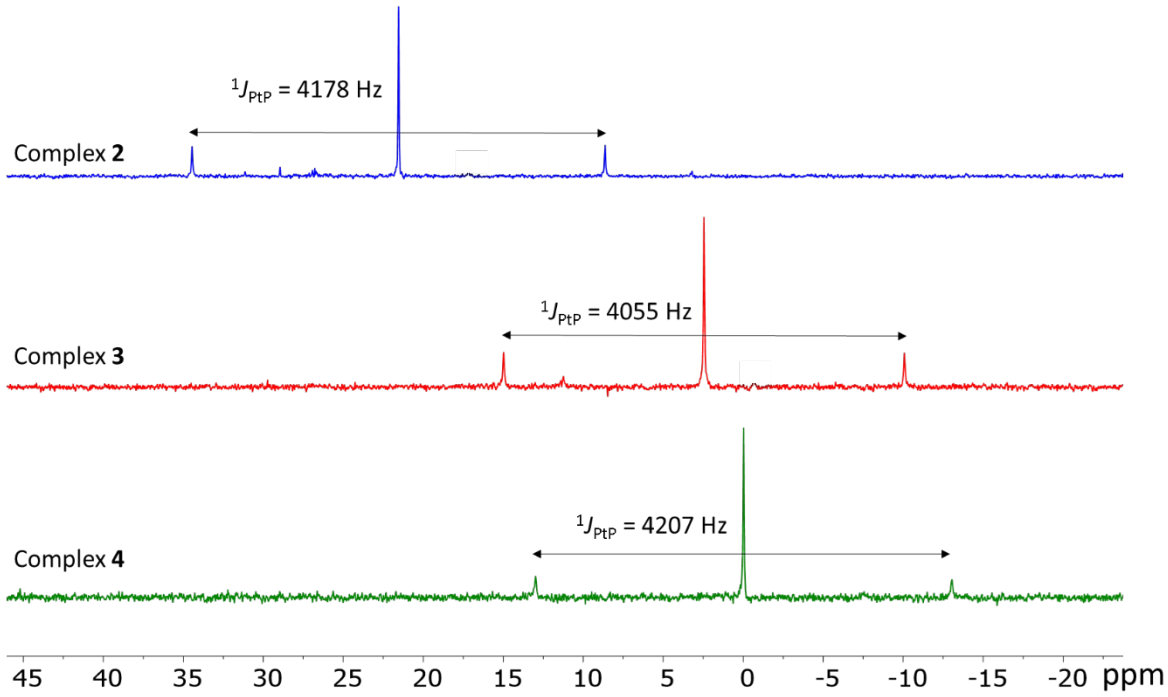

Fig. 1 $^{31}P\{^1H\}$ NMR spectra of the complexes **2**-**4**.

X- Ray Structure Determination

Suitable crystals for X-ray crystallography were grown by slow evaporation of concentrated chloroform, dichloromethane or acetone solution of the complexes. The structures obtained by X-ray crystallography technique for all the complexes are presented in Fig. 2 and the numerical data are summarized in Table 1 (see the caption of Fig. 2 for selected geometrical parameters). As shown in Fig. 2, all the solid state structures exhibit distorted four-coordinated square planar geometry around the platinum center. For complex **1** the structure proposed in Scheme 1 with the methyl group *trans* to the pyridyl ring of pbz ligand is

confirmed. The largest deviation from ideal square planar geometry belongs to the N2-Pt1-N1 angle at 79.2(3)° which is associated with the Pt(pbz) chelate ring. For the complex **2**, the bond angles of N1–Pt1–N2 and P1–Pt1–C13 are respectively 78.3° and 85.1° confirming the distorted square planar geometry. The chelating N^N bite angle is much smaller than 90°. As expected, the PPh_3 ~~group~~ is located *trans* to the ligating N of benzimidazole ring (Pt1–P1 = 2.223(2) Å) and the Me group is located *trans* to the ligating N of the pyridyl ring (Pt1–C13 = 2.057(5) Å) (See Fig. 2). The structure of complex **3** (L= PPh_2Me) is very similar to that of complex **2**. The structure of complex **4** confirms that "PtMe(pbz)" moieties are connected through the dppac bridging ligand in which the P-C-C-P fragment is almost linear. The terminal Me ligands are transoid in relation to each other. It should be noted that mono-bridged dppac complexes where a dppac molecule acts as a unique bridging ligand between two metal fragments are not common [59, 60].

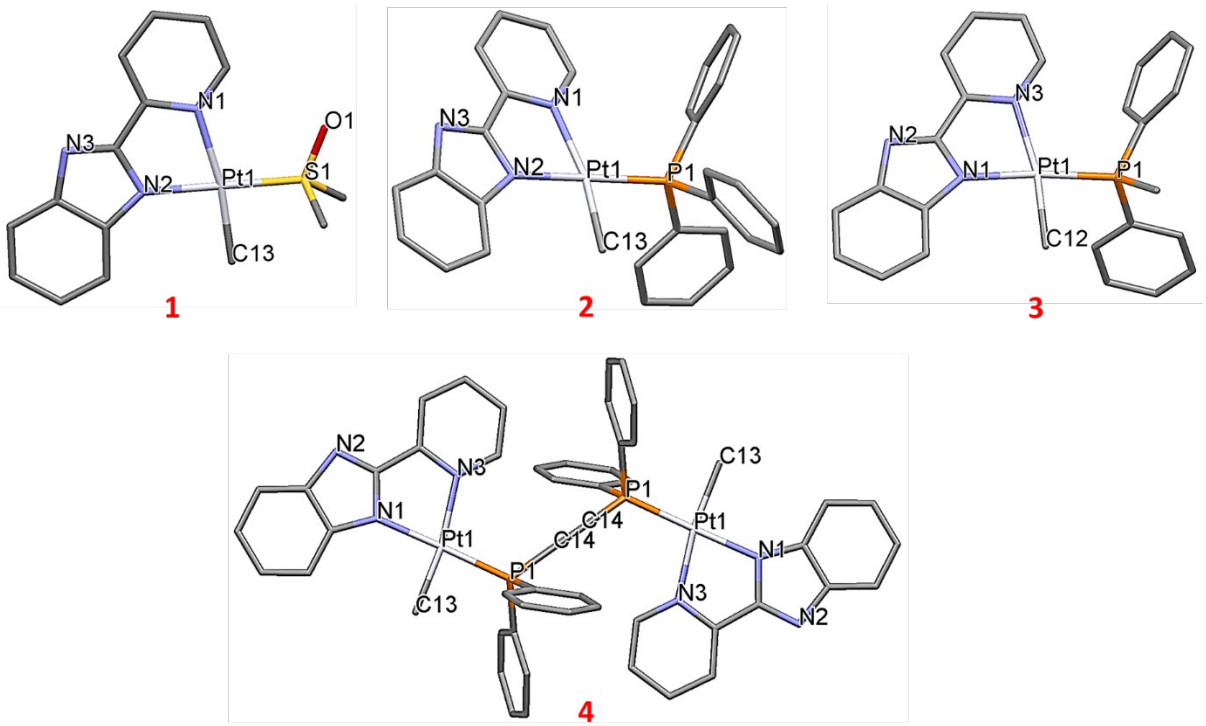

Fig. 2 (a) Structure of complexes **1-4**. All hydrogen atoms and solvent molecules (for complexes **1** and **3**) are omitted for clarity. Selected geometrical parameters (Å, deg.): Complex **1**: Pt1-C13 2.048(9); Pt1-N1 2.142(7); Pt1-N2 2.038(8); Pt1-S1 2.187(3); C13-Pt1-N2 92.0(3); N1-Pt1-N2 79.2(3); C13-Pt1-S1 89.1(3); S1-Pt1-N1 99.8(2); S1-Pt1-N2 175.9(2), Complex **2**: Pt1-N1 2.165(4); Pt1-N2 2.070(6); Pt1-P1 2.223(2); Pt1-C13 2.057(5); N1-Pt1-N2 78.3(2); P1-Pt1-C13 85.1(2); N1-Pt1-C13 169.6(2); P1-Pt1-N2 174.0(1), Complex **3**: Pt1-N1 2.072(6); Pt1-N3 2.156(5); Pt1-P1 2.218(2); Pt1-C12 2.057(7); N1-Pt-N3 78.4(2); C12-Pt1-N1 91.6(3); N3-Pt1-P1 104.92(16); P1-Pt1-C12 85.0(2), Complex **4**: Pt1-N1 2.069(5); Pt1-N3 2.142(6); Pt1-P1 2.2002(19); Pt1-C13 2.049(7); N1-Pt1-N3 78.7(2); P1-Pt1-C13 86.7(2); N1-Pt1-C13 92.2(13); P1-Pt1-N3 102.50(16).

ESI-MS results further confirm the molecular formulas ~~formation~~ by demonstrated isotopically well-resolved peaks at *m/z* = 667.16, 605.14 and 1203.23 which are respectively related to [**2**+H]$^+$, [**3**+H]$^+$ and [**4**+H]$^+$. All of these peaks matched well with their calculated theoretical isotope distributions (see Fig. 3).

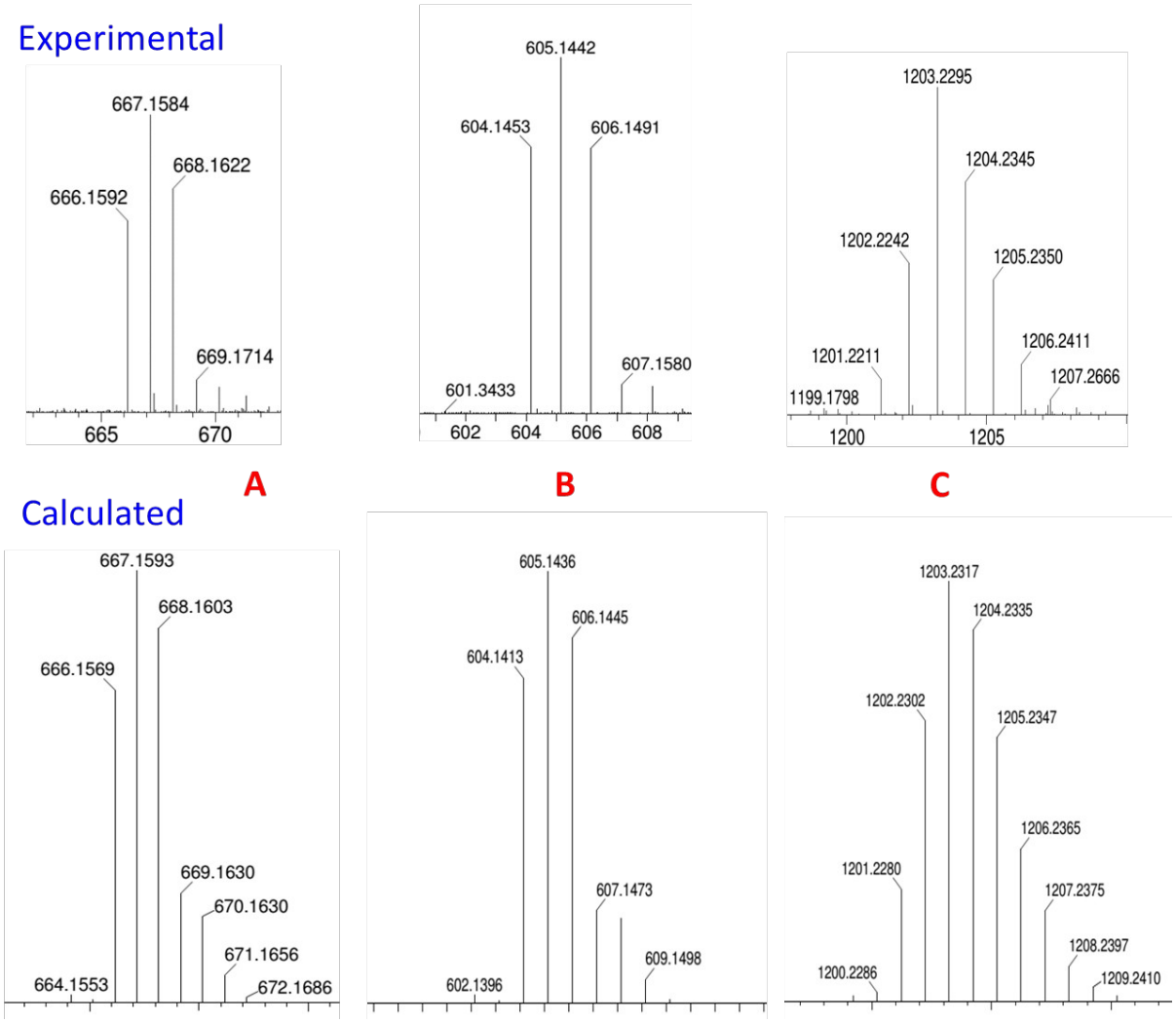

Fig. 3 Expanded (top) and simulated (bottom) isotopic pattern ESI-MS spectra of complexes [**2**+H]$^+$ (A), [**3**+H]$^+$ (B), and [**4**+H]$^+$ (C), showing the expected intensity due to isotopic distribution.

Photophysical Properties of Pt Complexes

Complexes **1-4** are stable in most ~~of~~ common organic solvents including acetone, CH_2Cl_2, $CHCl_3$ and CH_3CN ~~which allows~~thereby allowing ~~the~~ investigation of their photophysical properties in a wide range of solvents. Photophysical properties of these complexes were examined using their absorption and luminescence spectra in solid state and CH_2Cl_2 at 298 and 77 K, respectively.

Absorption spectra

Fig. 4 shows the absorption spectra recorded ~~of~~ for **1-4** in different solvents~~; . the~~ The numerical data including extinction coefficients are listed in Table 2. Free Hpbz in CH_2Cl_2 solvent has an intense absorption band with a mixmum at 310 nm which is attributed to a spin allowed intraligand ^{1}IL, π-π* transitions (Fig. S1).~~.~~ ~~For **1** this transition is highly shifted to 347 nm (see Fig. S1).~~ The major absorption for all of the ~~complexes centered~~platinum(II) complexes of pbz described here occurs at ~~around~~ ~350 nm in CH_2Cl_2 (Fig. 4E), for example, **1** has two absorption bands at λ_{max} values at 294 and 347 nm with molar absorption coefficients (ε) of 1.28×10^4 and 2.05×10^4 M^{-1} cm^{-1}, respectively. The UV-vis spectra of **2** and **4** show absorptions at 292 and 288 nm (ε = 2.00×10^3 and 2.31×10^4 M^{-1} cm^{-1} for **2** and **4**, respectively) and sharp absorption bands at 348 and 349 nm (ε = 2.40×10^3 and 2.82×10^4 M^{-1} cm^{-1} for **2** and **4**, respectively. However, for **3**, a shoulder at 292 nm (ε = 7.04×10^4 M^{-1} cm^{-1}) and a sharp peak at 362 nm (ε = 7.20×10^4 M^{-1} cm^{-1}) are observed. The UV-vis spectra of **1-4** in other solvents, as shown in Fig. 4A-D, are similar to those recorded in CH_2Cl_2 solutions.

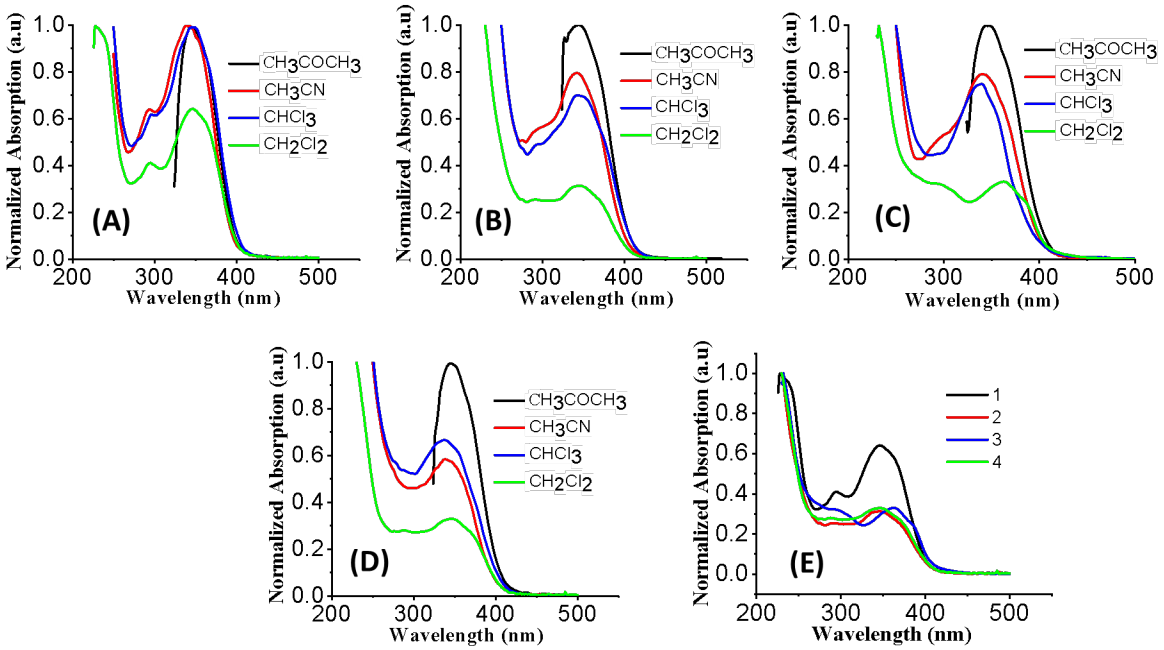

Fig. 4 UV-visible absorption spectra of complexes **1** (A), **2** (B), **3** (C) and **4** (D) ~~at~~ in different solvents (**1**: 7.8 × 10^{-6} M, **2**: 5.0 × 10^{-5} M, **3**: 1.3 × 10^{-5} M, **4**: 7.8 × 10^{-6} M) and complexes **1-4** in CH_2Cl_2 at 298 K (E). UV cutoff of acetone is 330 nm.

In order to gain further insight into the nature of electronic transitions in the complexes **1-4** (CH_2Cl_2), TD-DFT calculations were performed on the optimized ground state geometries. As shown in Fig. 5, the computed absorption wavelengths (bars) in CH_2Cl_2 are in good agreement with their corresponding experimental spectra. The numerical data for the selected calculated wavelengths together with their assignments are listed in Table 2. For the complexes **1-4,** the plots of molecular orbitals are respectively shown in Fig S2-S5. The energies of the selected molecular orbitals in S_0 state for **1-4** together with their compositions in terms of ligands and metals are listed in Table S1. According to these calculations, the bands at ~350 nm are intraligand (IL)

bands red-shifted from that of the free ligand, although for complex 4, this band also has an admixture of ~~The~~ LLCT character. The relatively intense electronic transitions at higher energies (below 295 nm) are ~~normally~~ attributed to MLCT (for **1**, **3** and **4**; L= pbz) and ML″CT (for **3** and **4**; L″ = PPh_2Me and dppac) transitions. For the complex **1** a transition attributed to "ligand to ligand charge transfer" (L′LCT; L′= Me) is also observed. At higher energies, the electronic transitions of complex **2** is assigned to ligand to ligand charge transfer (LL″CT; L″ = PPh_3) and metal to ligand charge transfer (MLCT). ~~**The absorption bands, having high intensities and absorption coefficients (ε > 2.40×10³ M⁻¹ cm⁻¹), are observed for all the complexes around 350 nm (see Figure 4 and Table 2 for details).**~~

Table 2. TD-DFT computed spectra and experimental ~~ωαωελενγτη~~ λ_{max} values ~~(nm)~~ for the complexes **1-4**, at the ground state geometry in CH_2Cl_2 (1.0×10^{-4} M) solution (only transitions with a probability higher than 20% are reported).

λ_{cal} (f)[a]	λ_{max}(exp)[a,b]	Transitions (probability)	Assignments
1			(L=pbz, L′=Me, L″=DMSO)
284 (0.216)	294	HOMO-3 – LUMO (54) HOMO-1 – LUMO+1 (24)	MLCT/L′LCT IL
345 (0.411)	347	HOMO-1 – LUMO (95)	IL
2			(L=pbz, L′=Me, L″=PPh_3)
296 (0.224)	292	HOMO-1 – LUMO+2 (54) HOMO-3 – LUMO (22)	IL/ LL″CT/MLCT IL/ L′LCT
351 (0.413)	348	HOMO-1 – LUMO (90)	IL

3			(L=pbz, L′=Me, L′′=PPh_2Me)
293(0.083)	292	HOMO-2 – LUMO+1 (35) HOMO-2 – LUMO+3 (22)	MLCT/ ML′′CT MLCT/ML′′CT
350 (0.413)	362	HOMO-1 – LUMO (92)	IL
4			(L=pbz, L′=Me, L′′=dppac)
294 (0.186)	288	HOMO-5 – LUMO+1 (33)	MLCT/ ML′′CT
353 (0.634)	349	HOMO-2 – LUMO+1 (35) HOMO-3 – LUMO (34)	LL′′CT/ LLCT LL′′CT/ LMCT/ LLCT

[a] in nm. [b]Experimental spectra recorded in CH_2Cl_2.

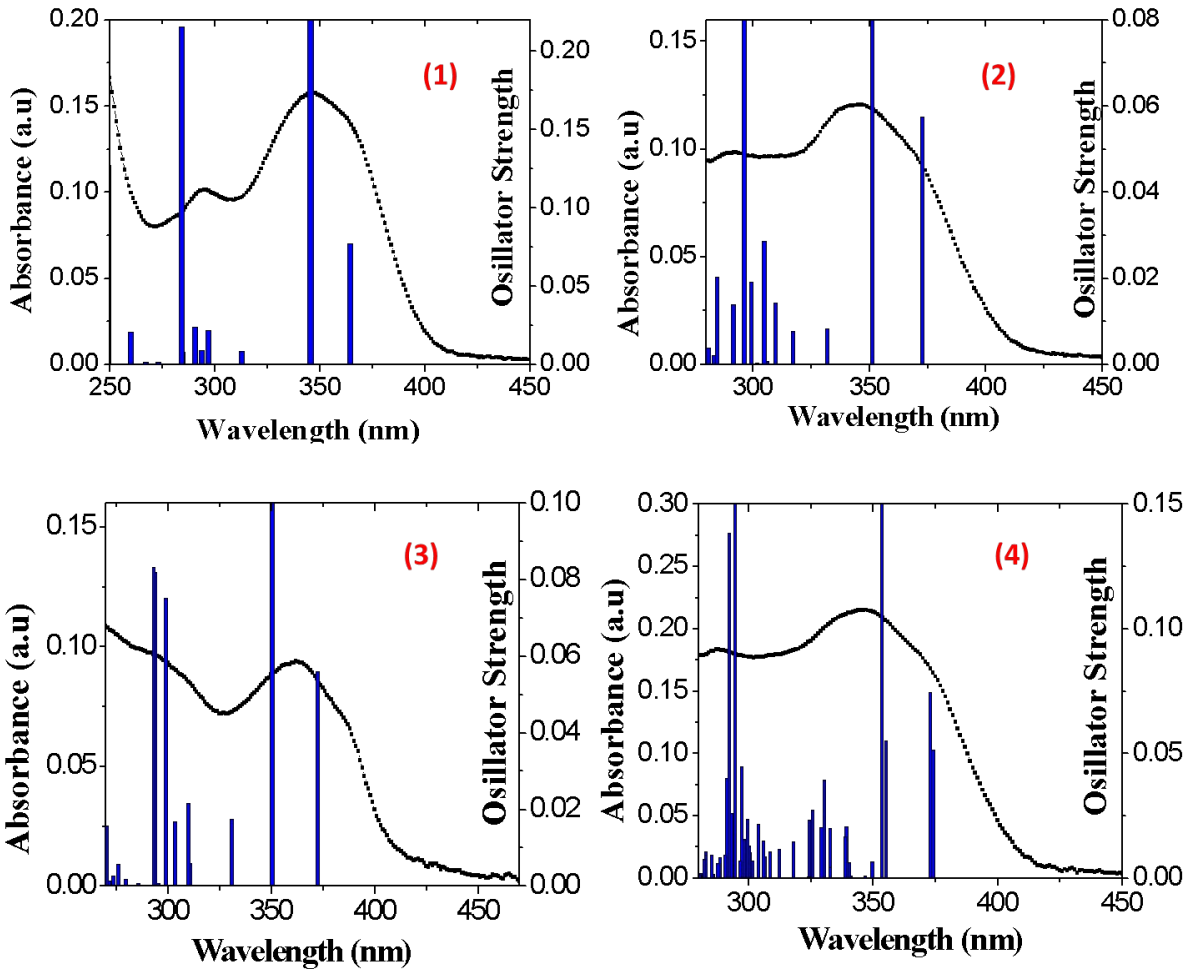

Fig. 5 Overlaid experimental absorbance (spectra) and calculated TD-DFT (bars) for the complexes **1-4**.

Emission spectra and DFT Investigations

~~All~~ Each of the complexes exhibits luminescence in the visible region in CH_2Cl_2 solvent as well as in the solid state at both room (298 K) and low (77 K) temperatures. The numerical data for the emission and excitation spectra of all the complexes are collected in Table 3. In addition, theoretical investigations (DFT and TD-DFT) were performed to provide insight into the photophysical behaviors of the studied complexes. The calculated wavelengths for the triplet transitions together with their characters in solid phase and CH_2Cl_2 solution are collected in Tables 4 and S3, respectively. Also, the emission spectra of the complexes **1-4** in CH_2Cl_2 are shown in Fig. 6A. The emission bands for the complexes **1–4** (see Table 3) are red shifted with respect to that for free ligand which is indicative of the effect of heavy metal and spin-orbit coupling on emission leading to triplet excited states. In this regard, the relatively long lifetime values (≥ 11.7 μs at 298 K) reveal that there is substantial spin-forbidden character in their emissive excited state [61].

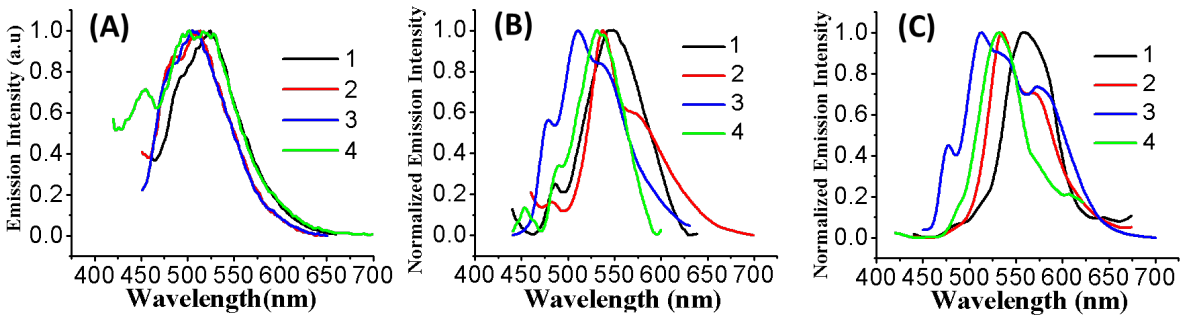

Fig. 6 Emission spectra of complexes 1-4 in deoxygenated CH_2Cl_2 solvent (A). Normalized emission spectra in solid state for the complexes **1-4** at room temperature (B) and 77 K (C).

Complexes **1-4** show a strong, visible emission band around 500 to 527 nm in room temperature dichloromethane with the respective maxima for **1**, **2**, **3** and **4** at ~524, 513, 505 and 527 nm. There are also three less intense shoulders in 492, 486, 481 and 459 nm, respectively, which could be assigned to vibronic progression peaks. The respective emission lifetimes measured at the peak maxima were found to be 26.8, 36.5, 11.7 and 15.4 μs, consistent with a triplet excited state phosphorescence. The absolute emission quantum yields (QY) found to be 7.2, 1.3, 2.9 and 4.7%, respectively. The highest QY value belongs to the complex **1** (with DMSO ligand) compared to the complexes **2-4** (with phosphine ligands).

Complexes **1-4** in the solid state are green emitters at 298 and 77 K (see Fig. 6B and C), in the range of 510-540 nm, displaying a structured emission band with the energy order **1** (549 nm) < **2** (537 nm) < **4** (532 nm) < **3** (511 nm), indicating a substantial involvement of pbz ligand in the emissive state.

In the wavelength region 450-500, the emission occurred on less intense peaks. For the complexes **1-3**, the emission bands (as confirmed by DFT/TD-DFT calculations) can be ~~originated from a typical~~attributed to transitions with mixed ^{3}IL ~~(intra-ligand center), and~~ ^{3}MLCT ~~(metal to ligand center)~~ and ^{3}LMCT character (in case of **1** and **2**) with vibronic

structure**.** The emission character of complex **4** was assigned as ^{3}IL, ^{3}LL″CT and ^{3}ML″CT (L″ = dppac).

Upon cooling to 77 K, intensities of the emission bands were increased while the band shapes remained similar to room temperature bands with a negligible blue shift for the complex **2**, and red shifts for the complexes **1** and **3**. This observation could be attributed to the enhanced structural rigidity in frozen state compared to room temperature [62] (see Fig. 6C and Table 3). To gain further insight into the nature of emission characters of **1-4**, in dichloromethane solution and in the solid state, DFT and TD-DFT calculations were performed for all the complexes. The structures of complexes **1-4**, with all having singlet (S_0) and triplet (T_1) states were optimized. Typically selected calculated bond distances and angles based on DFT optimized geometry for complex **2**, are shown in Fig. S6. As can be seen, the calculated structure gives band distance and angle values very close to those obtained for the related X-ray diffraction results (see Fig. S6 and 2 respectively). Energies of the important molecular orbitals for the complex **1-4**, in T_1 (including LSOMO and HSOMO which stand for “lowest singly occupied molecular orbital” and “highest singly occupied molecular orbital”, respectively) states were calculated. Energies of the selected molecular orbitals of the complexes **1-4** and their compositions in the excited state are reported in Table S2.

Table 3. Photophysical data of complexes **1-4** in different media.

Complex	Media	λ_{em}/nm (λ_{ex}/nm)	λ_{abs}/nm (log ε /$M^{-1}cm^{-1}$)	τ_{em}(μs)	Φ_{PL}(%)

Free Hpbz	CH_2Cl_2 (10^{-7} M)	307, 365$_{max}$, (300-500)	310(3.68)		
	Solid (298K)	358$_{max}$, 368, 485 (300-500)			
1	CH_2Cl_2 (10^{-5} M), 298 K	492, 524$_{max}$, (300-600)	294(4.10), 347(4.31)	26.8	7.2
	CH_2Cl_2 (10^{-5} M), 77 K	493 , 526 $_{max}$, (300-600)			
	Solid (298K)	486, 549$_{max}$ (320-600)			
	Solid (77K)	485, 558$_{max}$(320-600)			
2	CH_2Cl_2 (10^{-5} M), 298 K	486,513$_{max}$ (320-600)	292(3.30), 348(3.38)	36.5	1.3
	CH_2Cl_2 (10^{-5} M), 77 K	490, 510 $_{max}$, 425 (320-600)			
	Solid (298K)	487, 537$_{max}$, 577 (320-600)			
	Solid (77K)	535$_{max}$, 570 (320-600)			
3	CH_2Cl_2 (10^{-5} M), 298 K	481, 505$_{max}$, (320-600)	292(4.84), 362(4.85)	11.7	2.9
	CH_2Cl_2 (10^{-5} M), 77 K	482, 506$_{max}$, (320-600)			
	Solid (298K)	478, 511$_{max}$, 540 (320-600)			
	Solid (77K)	477, 513$_{max}$, 541, 573 (320-600)			
4	CH_2Cl_2 (10^{-5} M), 298 K	456, 512 $_{max}$ (320-600)	288(4.36), 349(4.45)	15.4	4.7
	CH_2Cl_2 (10^{-5} M), 77 K	458, 510max (320-600)			
	Solid (298K)	453, 490, 532$_{max}$ (320-600)			
	Solid (77K)	488, 532$_{max}$, 571 (320-600)			

Table 4. TD-DFT calculated transition wavelengths and main components of the triplet excited states of complexes **1-4**, based on optimized T_1 geometry in solid state (only transitions with a probability higher than 20% are reported).

Complex	Calc. (exp.) / nm	Configuration (Percentage Contribution.)	Transition character
1			(L=pbz, L″=DMSO)
	453(486)	LSOMO-1 – HSOMO (62)	IL, LMCT
		LSOMO – HSOMO (27)	IL, MLCT

	486(549)	LSOMO – HSOMO (58)	IL, MLCT
		LSOMO-1 – HSOMO (28)	IL, LMCT
2			(L=pbz, L″=PPh_3)
	473(487)	LSOMO-1 – HSOMO (50)	IL, LMCT
		LSOMO – HSOMO (40)	IL, MLCT
	500(537)	LSOMO – HSOMO (46)	IL, MLCT
		LSOMO-1 – HSOMO (40)	IL, LMCT
3			(L=pbz, L″=PPh_2Me)
	470(478)	LSOMO-1 – HSOMO (48)	IL
		LSOMO – HSOMO (44)	IL, MLCT
	497(511)	LSOMO – HSOMO (44)	IL, MLCT
		LSOMO-1 – HSOMO (44)	IL
4			(L=pbz, L″=dppac)
	467(453)	LSOMO-1 – HSOMO+3 (26)	LL″CT, IL, ML″CT
	496(490)	LSOMO – HSOMO+3 (24)	IL, LL″CT, ML″CT
	503(532)	LSOMO-2 – HSOMO+2 (24)	IL, LL″CT, ML″CT

Typical MO plots are shown in Table 5. Analysis of the frontier molecular orbitals reveals that the maximum contribution in the HOMO (the highest occupied molecular orbital) belongs to the benzimidazole moiety π_z for **1-4** with small contribution of platinum d orbitals (d_{xz} for **1-3** and d_{x2-y2} for **4**). Also, the results show that LUMO (lowest unoccupied molecular orbitals) in all complexes is significantly localized on the pyridyl ring with some contribution of dppac ligand in **4**. According to the TD-DFT calculation ~~in~~ of the triplet state in the gas phase, the singularly occupied molecular orbital (LSOMO for **1-3** and LSOMO-2 for **4**) is localized on the benzimidazole (p_z) with small contribution of platinum d orbitals (d_{xz} for **1** and **3**, d_{yz} for **2** and **4**).

As mentioned in the Introduction, compared to Pt(N^C^-) moiety, the photophysical properties of complexes having Pt(N^N^-) have not been widely investigated. As shown in Scheme 1, only one geometric isomer is obtained for complexes **1-4**. This suggests that the two nitrogen donor sites have a very different natures and *trans* influences, reinforcing the

comparison with N^C- cyclometalated ligands. In order to gain further insight into the effect of the (N^N-) ligand on the luminescence of the complexes, ~~a comparative study was~~ we compared ~~performed for~~the properties of complexes ~~[PtMe(PPh$_3$)(pbz)], **2**,~~ and ~~[PtMe(PPh$_2$Me)(pbz)],~~ **3**, with their (N^C-) analogues [PtMe(PPh$_3$)(ppy)], **7**, and [PtMe(PPh$_2$Me)(ppy)], **8**, in which ppy is 2-phenylpyridinate (see Fig. 7).[63] Although the complex **2** shows emission bands in solid state and CH_2Cl_2 solution, the ~~analogue~~ analoguus ppy complex, **7** is not emissive ~~in both~~either in the solid state ~~and~~ or CH_2Cl_2 solution at room (298 K) and low temperatures (77 K). On the other hand, complex **8** has an emission band at 476 nm with a vibronic progression at 507 nm and a shoulder at 540 nm in solid state at room temperature. The main band in the complex **8** is blue shifted compared to the complex **3** (507 and 511 nm for complexes **8** and **3**, respectively). Similarly, the less intense band ~~with less intense~~ is highly blue shifted (476 and 478 nm in complexes **8** and **3**, respectively; see Fig. 7) in the solid state at room temperature from the values seen in solution??. The shoulder band in both complexes is located at 540 nm. It is reported that the complex **8** has mainly ^{3}ILCT character mixed with some ^{3}MLCT character (L = cyclometalated ligand) in their emissive state. [63] The observation is similar to complex **3** with the same character for emission bands. In the case of complex **3**, there is a clear ^{3}IL pbz transition from the benzimidazole ring to pyridine ring, with some contributions of metal to ligand charge transfer ^{3}MLCT (see Table 5). Upon cooling of the solid samples to 77 K, the emission for both complexes **8** and **3** becomes more intense and better structured with negligible shifts

in wavelengths, compared to 298 K. There is a new emission band at 573 nm for complex **3**, compared to room temperature. The patterns for emission spectra of complexes **3** and **8**, at higher energies are ~~nearly~~ similar to each other as these complexes have the same origin and destination of transitions. In both complexes, the observed transitions are attributed to metal and central ligand (pbz and ppy in complexes **3** and **8**, respectively) as the origin of transitions to the pyridine moieties in pbz and ppy.

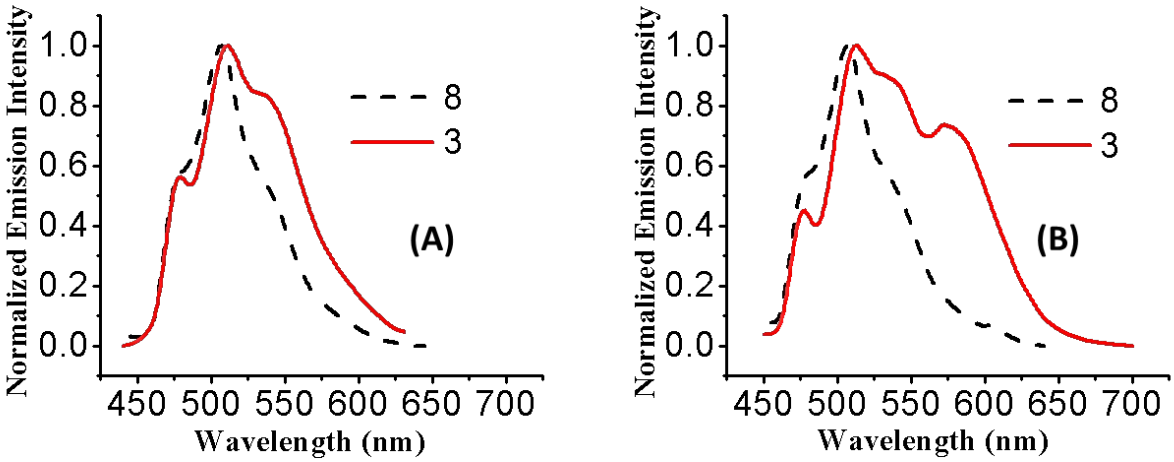

Fig. 7 Normalized emission spectra of complexes [PtMe(PPh_2Me)(ppy)], **8**, and [PtMe(PPh_2Me)(pbz)], **3**, in solid state at room temperature (**A**) and 77 K (**B**).

Table 5. Typical MO plots of the complexes **1-4**.

Orbitals	Complex **1**	Complex **2**	Complex **3**	Complex **4**
	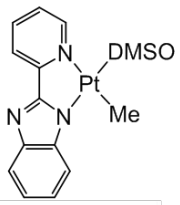	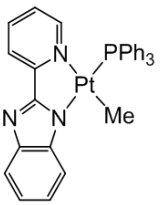	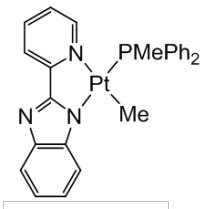	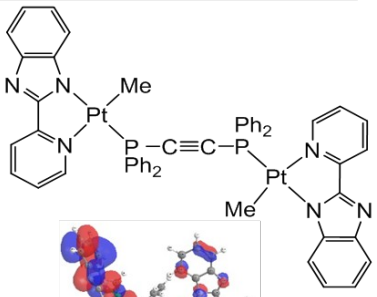
HOMO	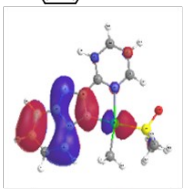	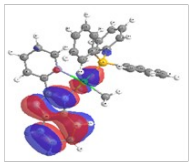	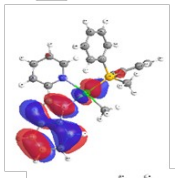	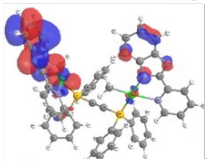
LUMO	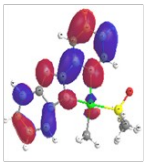	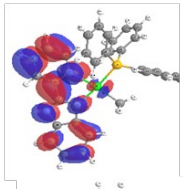	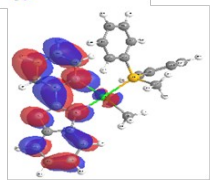	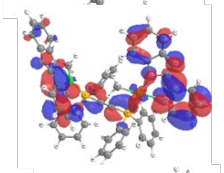
LSOMO	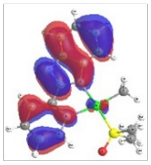	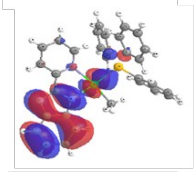	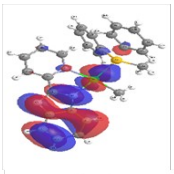	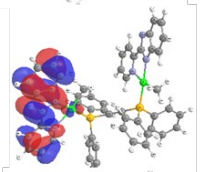
HSOMO	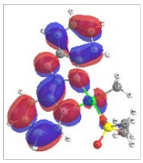	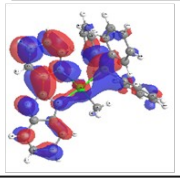	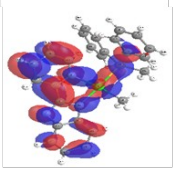	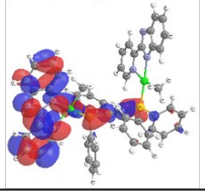

A cComparative HOMO-LUMO gap diagram for the complexes **1-4** is shown in Fig. 8. The HOMO-LUMO gap for the complexes **1**, **2**, **3** and **4**, are very close to each othersimilar (being 4.01, 3.93, 3.94, 3.90 eV, respectively), consistent with the similarity of their spectra. The values for the complexes **2** and **3** (3.93 and 3.94 eV respectively) are relatively somewhat red shifted in comparison to that of complex **1**. This observation is in agreement with the trend observed in experimental absorption spectra of the complexes (see above).

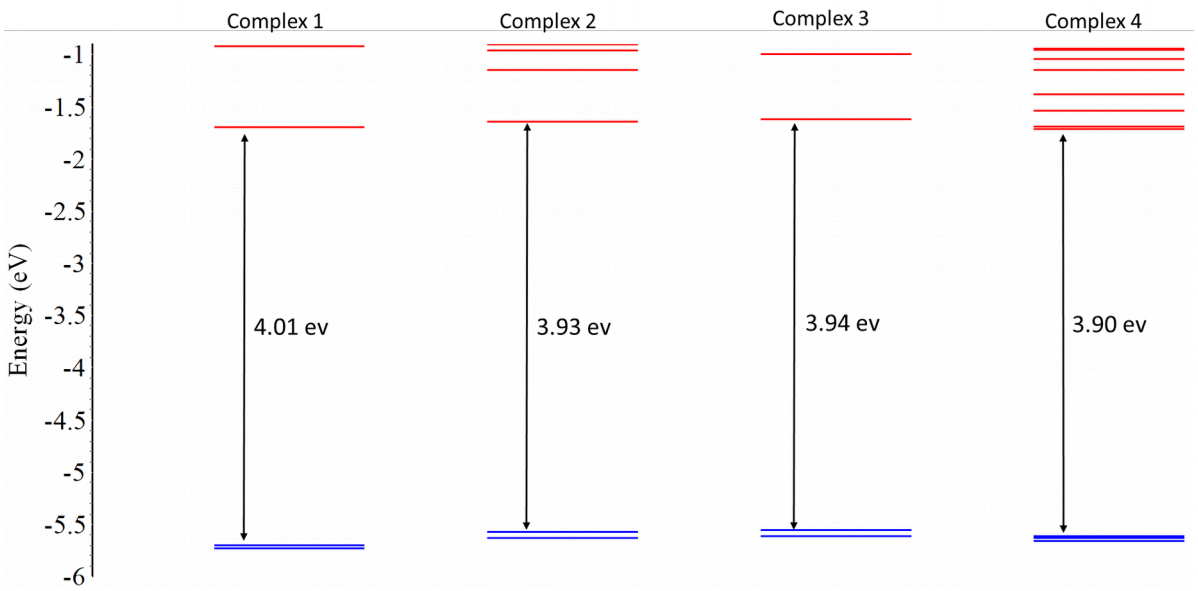

Fig. 8 Comparative energy level diagrams for the calculated MOs of complexes **1-4**.

In this work, we investigated emission properties of the complex **1-4** by optimization of their lowest-energy triplet state (T_1) using B3LYP method. Calculated emission wavelengths (the difference between ground state and excited state)[21] are 503, 512, 557, 515 nm (gas phase) for the complexes **1-4** respectively, which are ~~almost~~ close to the experimental values ~~achieved for them~~recorded (540, 537, 540, 530 nm for complexes **1**, **2**, **3** and **4**, respectively, in solid).

Conclusions

A series of mononuclear platinum(II) complexes, with the general formula [Pt(Me)(pbz)(L)], in which L = DMSO (**1**), PPh_3 (**2**), PPh_2Me (**3**) are prepared. The reaction of complex **1** with bis(diphenylphosphino)acetylene (= dppac) in 1:0.5 molar ratio gives a

binuclear Pt(II) complex [Pt_2Me_2(μ-dppac)$(pbz)_2$], **4**. Photophysical properties of these complexes were investigated experimentally in solid state and solution (degassed dichloromethane) at 298 and 77 K and confirmed by TD-DFT calculations. The ambient temperature emission life times of the complexes are in order of μs. Triplet excited ~~states~~ state assignments ~~responsible~~ for the observed phosphorescence emission of the complexes **1-4** are supported by DFT/TD-DFT calculations and assigned to transitions with mixed ^{3}IL/^{3}LMCT/^{3}MLCT in which L = pbz, for the complexes **1-3**, and ^{3}IL/^{3}LLCT/^{3}LL′′CT/^{3}ML′′CT (L′′ = dppac) for the complex **4**. Solid state emission band for the complexes **1-4**, shows a red shift related to the corresponding solution, which may be attributed to the contribution of some excimeric character due to the occurrence of π···π intermolecular interactions in the solid state.[27]

The comparison between [PtMe(PPh_3)(pbz)], **2**, and [PtMe(PPh_2Me)(pbz)], **3**, with their (N^C$^-$) analogues [PtMe(PPh_3)(ppy)], **7**, and [PtMe(PPh_2Me)(ppy)], **8**, reveals that while the complex **2** shows emission bands in solid state and CH_2Cl_2 solution, the analogue ppy complex, **7** is not emissive either in ~~both~~ the solid state ~~and~~ or in CH_2Cl_2 solution at different temperatures. Complex **8** has mainly ^{3}ILCT character mixed with some ^{3}MLCT character (L = cyclometalated ligand), similar to complex **3**, having the same character for emission bands.

Acknowledgments

We thank the Iran National Science Foundation (Grant No. 97012633), Shiraz University, the Islamic Azad University (Shiraz Branch) and

Department of Chemistry and Biochemistry at UCSB for financial support. We thank Dr. Hamidreza Shahsavari and Dr. Reza Babadi Aghakhanpour for reading and commenting on this manuscript before its submission for publication.

References

[1] K. Li, G.S.M. Tong, Q. Wan, G. Cheng, W.-Y. Tong, W.-H. Ang, W.-L. Kwong, C.-M. Che, Highly phosphorescent platinum (II) emitters: photophysics, materials and biological applications, Chem. Sci., 7 (2016) 1653-1673.
[2] P.-H. Lanoë, A. Moreno-Betancourt, L. Wilson, C. Philouze, C. Monnereau, H. Jamet, D. Jouvenot, F. Loiseau, Neutral heteroleptic cyclometallated Platinum (II) complexes featuring 2-phenylbenzimidazole ligand as bright emitters in solid state and in solution, Dyes and Pigm., 162 (2019) 967-977.
[3] Q. Zhao, C. Huang, F. Li, Phosphorescent heavy-metal complexes for bioimaging, Chem. Soc. Rev., 40 (2011) 2508-2524.
[4] T.-Y. Li, X. Liang, L. Zhou, C. Wu, S. Zhang, X. Liu, G.-Z. Lu, L.-S. Xue, Y.-X. Zheng, J.-L. Zuo, N-heterocyclic carbenes: versatile second cyclometalated ligands for neutral iridium (III) heteroleptic complexes, Inorg. Chem. , 54 (2014) 161-173.
[5] I. Omae, Applications of five-membered ring products of cyclometalation reactions as anticancer agents, Coord. Chem. Rev., 280 (2014) 84-95.
[6] J.G. Williams, S. Develay, D.L. Rochester, L. Murphy, Optimising the luminescence of platinum (II) complexes and their application in organic light emitting devices (OLEDs), Coord. Chem. Rev. , 252 (2008) 2596-2611.
[7] H. Xu, R. Chen, Q. Sun, W. Lai, Q. Su, W. Huang, X. Liu, Recent progress in metal–organic complexes for optoelectronic applications, Chem. Soc. Rev. , 43 (2014) 3259-3302.
[8] J. Demas, B. DeGraff, Applications of luminescent transition platinum group metal complexes to sensor technology and molecular probes, Coord. Chem. Rev. , 211 (2001) 317-351.
[9] T.N. Nguyen, F.M. Ebrahim, K.C. Stylianou, Photoluminescent, upconversion luminescent and nonlinear optical metal-organic frameworks: From fundamental photophysics to potential applications, Coord. Chem. Rev. , 377 (2018) 259-306.
[10] D. Qiu, M. Li, Q. Zhao, H. Wang, C. Yang, Cyclometalated Platinum (II) Terpyridylacetylide with a Bis (arylamine) Donor as a Proton-Triggered Luminescence Chemosensor for Zn^{2+}, Inorg. Chem., 54 (2015) 7774-7782.
[11] G. Turnbull, J.G. Williams, V.N. Kozhevnikov, Rigidly linking cyclometallated Ir (III) and Pt (II) centres: an efficient approach to strongly absorbing and highly phosphorescent red emitters, Chem. Comm. , 53 (2017) 2729-2732.
[12] M.H.-Y. Chan, M. Ng, S.Y.-L. Leung, W.H. Lam, V.W.-W. Yam, Synthesis of luminescent Platinum (II) 2, 6-bis (N-dodecylbenzimidazol-2′-yl) pyridine foldamers and their supramolecular assembly and metallogel formation, J. Am. Chem. Soc. , 139 (2017) 8639-8645.
[13] W. Zhang, F. Zhang, Y.-L. Wang, B. Song, R. Zhang, J. Yuan, Red-emitting ruthenium (II) and iridium (III) complexes as phosphorescent probes for methylglyoxal in vitro and in vivo, Inorg. Chem. , 56 (2017) 1309-1318.

[14] K.Y. Zhang, P. Gao, G. Sun, T. Zhang, X. Li, S. Liu, Q. Zhao, K.K.-W. Lo, W. Huang, Dual-Phosphorescent Iridium(III) Complexes Extending Oxygen Sensing from Hypoxia to Hyperoxia, J. Am. Chem. Soc. , 140 (2018) 7827-7834.
[15] Z. He, M. Li, W. Que, P.J. Stang, Self-assembly of metal-ion-responsive supramolecular coordination complexes and their photophysical properties, Dalton Trans., 46 (2017) 3120-3124.
[16] M. Zhang, M.L. Saha, M. Wang, Z. Zhou, B. Song, C. Lu, X. Yan, X. Li, F. Huang, S. Yin, P.J. Stang, Multicomponent platinum (II) cages with tunable emission and amino acid sensing, J. Am. Chem. Soc. , 139 (2017) 5067-5074.
[17] M.M. Mdleleni, J.S. Bridgewater, R.J. Watts, P.C. Ford, Synthesis, structure, and spectroscopic properties of ortho-metalated platinum (II) complexes, Inorg. Chem. , 34 (1995) 2334-2342.
[18] M. Fereidoonnezhad, B. Kaboudin, T. Mirzaee, R. Babadi Aghakhanpour, M. Golbon Haghighi, Z. Faghih, Z. Faghih, Z. Ahmadipour, B. Notash, H.R. Shahsavari, Cyclometalated Platinum (II) Complexes Bearing Bidentate O, O′-Di (alkyl) dithiophosphate Ligands: Photoluminescence and Cytotoxic Properties, Organometallics, 36 (2017) 1707-1717.
[19] H.R. Shahsavari, R. Babadi Aghakhanpour, M. Nikravesh, J. Ozdemir, M. Golbon Haghighi, B. Notash, M.H. Beyzavi, Highly Emissive Cycloplatinated (II) Complexes Obtained by the Chloride Abstraction from the Complex [Pt (ppy) (PPh_3)(Cl)]: Employing Various Silver Salts, Organometallics, 37 (2018) 2890-2900.
[20] M.S. Sangari, M.G. Haghighi, S.M. Nabavizadeh, A. Pfitzner, M. Rashidi, Influence of ancillary ligands on the photophysical properties of cyclometalated organoplatinum (ii) complexes, New J. Chem. , 42 (2018) 8661-8671.
[21] H. Molaee, S.M. Nabavizadeh, M. Jamshidi, M. Vilsmeier, A. Pfitzner, M.S. Sangari, Phosphorescent heterobimetallic complexes involving platinum (IV) and rhenium (VII) centers connected by an unsupported μ-oxido bridge, Dalton Trans., 46 (2017) 16077-16088.
[22] J.R. Berenguer, E. Lalinde, M.T. Moreno, Luminescent cyclometalated-pentafluorophenyl Pt^{II}, Pt^{IV} and heteropolynuclear complexes, Coord. Chem. Rev., 366 (2018) 69-90.
[23] F. Niroomand Hosseini, Determination of Reaction Kinetic Parameters from Variable Temperature Kinetic Study for Oxidative Addition Reaction on Binuclear Cyclometalated Platinum (II) Complexes, Inorg. Chem. Res. , 2 (2019) 26-31.
[24] S. Paziresh, R.B. Aghakhanpour, M. Rashidi, S.M. Nabavizadeh, Simple tuning of the luminescence properties of the double rollover cycloplatinated (II) structure by halide ligands, New J. Chem. , 42 (2018) 1337-1346.
[25] R.B. Aghakhanpour, S.M. Nabavizadeh, M. Rashidi, Newly designed luminescent di-and tetra-nuclear double rollover cycloplatinated (II) complexes, J. Organomet. Chem. , 819 (2016) 216-227.
[26] S. Paziresh, R. Babadi Aghakhanpour, S. Fuertes, V. Sicilia, F. Niroomand Hosseini, S.M. Nabavizadeh, A double rollover cycloplatinated(II) skeleton: a versatile platform for tuning emission by chelating and non-chelating ancillary ligand systems, Dalton Trans., 48 (2019) 5713-5724.
[27] G. Millán, N. Giménez, R. Lara, J.s.R. Berenguer, M.T. Moreno, E. Lalinde, E. Alfaro-Arnedo, I.P. López, S. Piñeiro-Hermida, J.G. Pichel, Luminescent Cycloplatinated Complexes with Biologically Relevant Phosphine Ligands: Optical and Cytotoxic Properties, Inorg. Chem., 58 (2019) 1657-1673.
[28] R.B. Aghakhanpour, S.M. Nabavizadeh, M. Rashidi, M. Kubicki, Luminescence properties of some monomeric and dimeric cycloplatinated (II) complexes containing biphosphine ligands, Dalton Trans., 44 (2015) 15829-15842.

[29] L. Schneider, V. Sivchik, K.-y. Chung, Y.-T. Chen, A.J. Karttunen, P.-T. Chou, I.O. Koshevoy, Cyclometalated platinum (II) cyanometallates: luminescent blocks for coordination self-assembly, Inorg. Chem. , 56 (2017) 4459-4467.
[30] S.R. Barzegar-Kiadehi, M. Golbon Haghighi, M. Jamshidi, B. Notash, Influence of the Diphosphine Coordination Mode on the Structural and Optical Properties of Cyclometalated Platinum (II) Complexes: An Experimental and Theoretical Study on Intramolecular Pt··· Pt and π··· π Interactions, Inorg. Chem. , 57 (2018) 5060-5073.
[31] A. Nahaei, S.M. Nabavizadeh, F.N. Hosseini, S.J. Hoseini, M.M. Abu-Omar, Arene CH bond activation and methane formation by a methylplatinum (II) complex: Experimental and theoretical elucidation of mechanism, New J. Chem. , 43 (2019) 6513-6522.
[32] S.O. Ojwach, A.O. Ogweno, M.P. Akerman, (Pyridyl) benzoazole palladium (II) complexes as homogeneous catalysts in hydrogenation of alkenes and alkynes, Catal. Sci. Tech. , 6 (2016) 5069-5078.
[33] T.K. Dey, K. Ghosh, P. Basu, R.A. Molla, S.M. Islam, Chloromethylated polystyrene immobilized ruthenium complex of 2-(2-pyridyl) benzimidazole catalyst for the synthesis of bioactive disubstituted ureas by carbonylation reaction, New J. Chem. , 42 (2018) 9168-9176.
[34] E. Guney, Y. Kaya, V.T. Yilmaz, S. Gumus, Synthesis, experimental and theoretical characterization of palladium (II) and platinum (II) saccharinate complexes with 2-(2-pyridyl) benzimidazole, Spect. Chim. Acta A: Mol. Biomol. Spect. , 79 (2011) 1171-1178.
[35] D. Peng, W. Zhang, G. Tang, J. Zhou, J. Hu, Q. Xie, C. Zhong, Novel dye sensitizers of main chain polymeric metal complexes based on complexes of 2-(2′-pyridyl) benzimidazole derivative with Zn (II), Co (II): synthesis, characterization, and photovoltaic performance for dye-sensitized solar cells, J. Iran. Chem. Soc. , 12 (2015) 397-404.
[36] M. Serratrice, M.A. Cinellu, L. Maiore, M. Pilo, A. Zucca, C. Gabbiani, A. Guerri, I. Landini, S. Nobili, E. Mini, Synthesis, structural characterization, solution behavior, and in vitro antiproliferative properties of a series of gold complexes with 2-(2′-pyridyl) benzimidazole as ligand: comparisons of gold (III) versus gold (I) and mononuclear versus binuclear derivatives, Inorg. Chem., 51 (2012) 3161-3171.
[37] Y. Chi, P.-T. Chou, Transition-metal phosphors with cyclometalating ligands: fundamentals and applications, Chem. Soc. Rev. , 39 (2010) 638-655.
[38] O.S. Wenger, Vapochromism in organometallic and coordination complexes: chemical sensors for volatile organic compounds, Chem. Rev. , 113 (2013) 3686-3733.
[39] M. Jamshidi, S.M. Nabavizadeh, H. Sepehrpour, F.N. Hosseini, R. Kia, M. Rashidi, Cycloplatinated (II) complexes containing bridging bis (diphenylphosphino) acetylene: Photophysical study, J. Lumin., 179 (2016) 222-229.
[40] N. Wang, J.-s. Lu, T.M. McCormick, S. Wang, Ru–Pt and Ru–Pd heterobimetallic complexes based on a new ligand with two distinct chelate sites, Dalton Trans., 41 (2012) 5553-5561.
[41] M. Serratrice, L. Maiore, A. Zucca, S. Stoccoro, I. Landini, E. Mini, L. Massai, G. Ferraro, A. Merlino, L. Messori, Cytotoxic properties of a new organometallic platinum (II) complex and its gold (I) heterobimetallic derivatives, Dalton Trans., 45 (2016) 579-590.
[42] Q.-D. Liu, W.-L. Jia, S. Wang, Blue luminescent 2-(2 ‘-Pyridyl) benzimidazole derivative ligands and their orange luminescent mononuclear and polynuclear organoplatinum (II) complexes, Inorg. Chem. , 44 (2005) 1332-1343.

[43] D. Qiu, Y. Guo, H. Wang, X. Bao, Y. Feng, Q. Huang, J. Zeng, G. Qiu, Synthesis, crystal structure, photophysical property and electropolymerization of Pt (II) complexes with carbazole-grafting 2-(2-pyridyl) benzimidazole, Inorg. Chim. Acta 14 (2011) 1520-1524.
[44] E. Guney, Y. Kaya, V.T. Yilmaz, S. Gumus, Synthesis, experimental and theoretical characterization of palladium (II) and platinum (II) saccharinate complexes with 2-(2-pyridyl) benzimidazole, Spect. Chim. Acta A 79 (2011) 1171-1178.
[45] M.-A. Haga, Synthesis and protonation-deprotonation reactions of ruthenium (II) complexes containing 2, 2′-bibenzimidazole and related ligands, Inorg. Chim. Acta 75 (1983) 29-35.
[46] W.L. Jia, T. McCormick, Y. Tao, J.-P. Lu, S. Wang, New Phosphorescent Polynuclear Cu (I) Compounds Based on Linear and Star-Shaped 2-(2 ‘-Pyridyl) benzimidazolyl Derivatives: Syntheses, Structures, Luminescence, and Electroluminescence, Inorg. Chem. , 44 (2005) 5706-5712.
[47] C. Zhong, R. Guo, Q. Wu, Design and syntheses of blue luminescent Cu (II) and Zn (II) polymeric complexes with 2-(2′-pyridyl) benzimidazole derivative ligand, Reac. Func. Poly. , 67 (2007) 408-415.
[48] W.-L. Jia, Y.-F. Hu, J. Gao, S. Wang, Linear and star-shaped polynuclear Ru(II) complexes of 2-(2′-pyridyl) benzimidazolyl derivatives: syntheses, photophysical properties and red light-emitting devices, Dalton Trans., (2006) 1721-1728.
[49] A. Kamecka, A. Kapturkiewicz, K. Suwińska, Luminescent osmium (II) complexes with 2-(2-pyridyl)-benzimidazolate anion, Inorg. Chem. Comm. , 89 (2018) 27-31.
[50] H. Yi, J.A. Crayston, J.T. Irvine, Ruthenium complexes of 2-(2′-pyridyl) benzimidazole as photosensitizers for dye-sensitized solar cells, Dalton Trans., (2003) 685-691.
[51] K. Wang, L. Huang, L. Gao, L. Jin, C. Huang, Synthesis, crystal structure, and photoelectric properties of Re $(CO)_3$ClL (L= 2-(1-ethylbenzimidazol-2-yl) pyridine), Inorg. Chem., 41 (2002) 3353-3358.
[52] N.M. Shavaleev, Z.R. Bell, T.L. Easun, R. Rutkaite, L. Swanson, M.D. Ward, Complexes of substituted derivatives of 2-(2-pyridyl) benzimidazole with Re (I), Ru (II) and Pt (II): structures, redox and luminescence properties, Dalton Trans., (2004) 3678-3688.
[53] F. Raoof, M. Boostanizadeh, A.R. Esmaeilbeig, S.M. Nabavizadeh, R.B. Aghakhanpour, K.B. Ghiassi, M.M. Olmstead, A.L. Balch, Reactivity comparison of five-and six-membered cyclometalated platinum (II) complexes in oxidative addition reactions, RSC Adv., 5 (2015) 85111-85121.
[54] G. Sheldrick, SADABS, Empirical Absorption Correction Program; University of Göttingen: Germany, 1997, (2005).
[55] SHELXTL PC, (Version 6.12, Bruker AXS Inc., Madison, WI, 2005).
[56] M. Frisch, G. Trucks, H.B. Schlegel, G. Scuseria, M. Robb, J. Cheeseman, G. Scalmani, V. Barone, B. Mennucci, G. Petersson, Gaussian 09, revision D. 01, Gaussian, Inc., Wallingford CT, 2009.
[57] P.J. Hay, W.R. Wadt, Ab initio effective core potentials for molecular calculations. Potentials for the transition metal atoms Sc to Hg, J. Chem. Phys. , 82 (1985) 270-283.
[58] L. Skripnikov, Chemissian: software to analyze spectra, build density maps and molecular orbitals, Version, 4 (2016).
[59] S.M. Nabavizadeh, F. Niroomand Hosseini, N. Nejabat, Z. Parsa, Bismuth–Halide Oxidative Addition and Bismuth–Carbon Reductive Elimination in Platinum Complexes Containing Chelating Diphosphine Ligands, Inorg. Chem. , 52 (2013) 13480-13489.

[60] L.R. Falvello, J. Forniés, J. Gómez, E. Lalinde, A. Martín, F. Martínez, M.T. Moreno, Some platinum (II) complexes containing bis(diphenylphosphino)acetylene PPh_2CCPPh_2: synthesis, characterisation and crystal structures, J. Chem. Soc. Dalton Trans., (2001) 2132-2140.
[61] H. Uesugi, T. Tsukuda, K. Takao, T. Tsubomura, Highly emissive platinum (II) complexes bearing carbene and cyclometalated ligands, Dalton Trans. , 42 (2013) 7396-7403.
[62] M. Jamshidi, S.M. Nabavizadeh, H.R. Shahsavari, M. Rashidi, Photophysical and DFT studies on cycloplatinated complexes: modification in luminescence properties by expanding of π-conjugated systems, RSC Adv., 5 (2015) 57581-57591.
[63] H.R. Shahsavari, R.B. Aghakhanpour, M. Babaghasabha, M.G. Haghighi, S.M. Nabavizadeh, B. Notash, Photophysical properties of a series of cycloplatinated (II) complexes featuring allyldiphenylphosphane, New J. Chem. , 41 (2017) 3798-3810.